# A "Multimessenger" Approach to Substructure Lensing

Chuck Keeton

July 22, 2009

# Substructure lensing

Past.

- Mao & Schneider 1998: connect flux ratios and substructure
- Metcalf & Madau 2001, Chiba 2002: propose to test CDM
- Dalal & Kochanek 2002: constrain substructure mass fraction

Present/future.

- New observables.
- Can we learn more about substructure?
- Is there really a population of clumps?
- Can we constrain its: mass function? spatial distribution? redshift evolution?
- What does it reveal about dark matter?

# Flux ratio anomalies

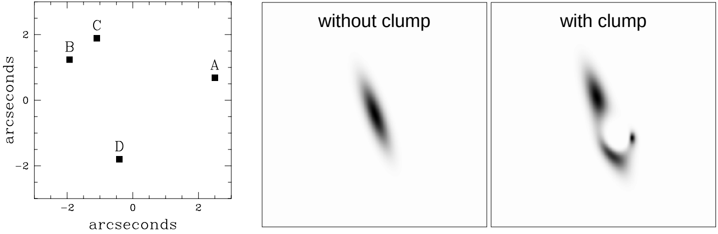


Flux ratio anomalies are hard to miss, and hard to misinterpret.

*(CRK, Gaudi & Petters 2003, 2005; Congdon & CRK 2005; Yoo et al. 2005, 2006)*

# B1555+375

Marlow et al. (1999)

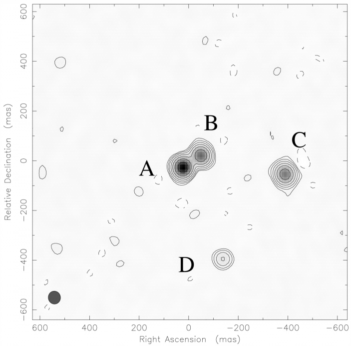


Smooth models generically predict $A - B \approx 0$. *(CRK, Gaudi & Petters 2005)*

# B2045+265

Fassnacht et al. (1999)

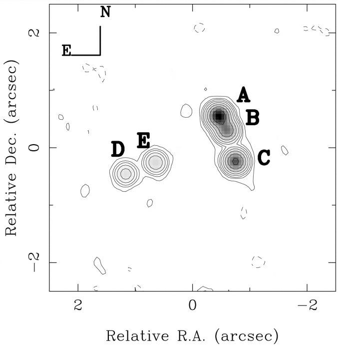


Smooth models predict $A - B + C \approx 0$. *(CRK, Gaudi & Petters 2003)*

# Flux ratios and substructure

Dalal & Kochanek (2002): constrain substructure mass fraction

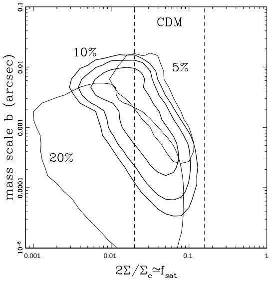


Single-wavelength flux ratios reveal

$$\int m \, \frac{dN}{dm} \, dm$$

but say little about $dN/dm$ itself.

# Finite source effects

Flux perturbation depends on size of subhalo relative to size of source. *(Dobler & CRK 2006)*

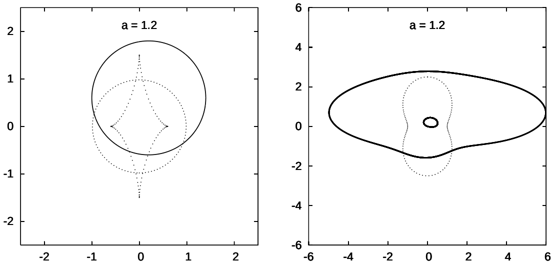

# Finite source effects

Flux perturbation depends on size of subhalo relative to size of source. *(Dobler & CRK 2006)*

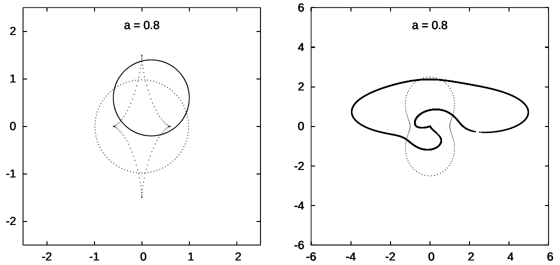

# Finite source effects

Flux perturbation depends on size of subhalo relative to size of source. *(Dobler & CRK 2006)*

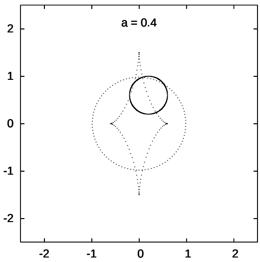


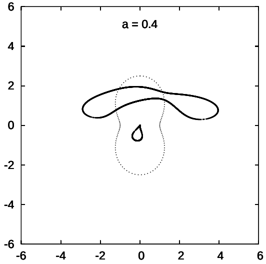

# Finite source effects

Flux perturbation depends on size of subhalo relative to size of source. *(Dobler & CRK 2006)*

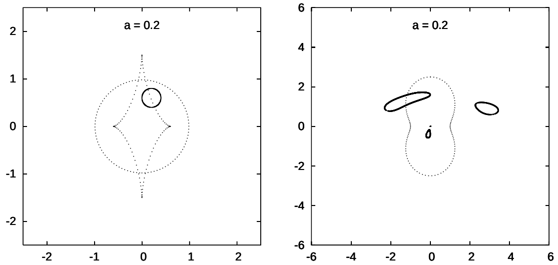

# Finite source effects

*(Dobler & CRK 2006)*

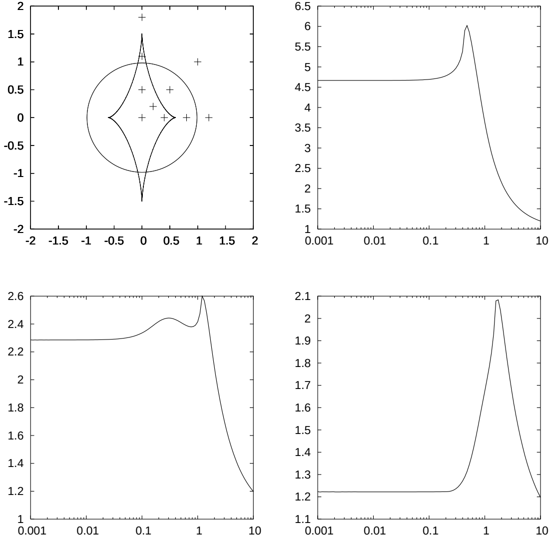

# Multiwavelength flux ratios

Heuristically, each wavelength probes substructure above some mass threshold:

$$\delta\mu(\lambda) \sim \int_{m(R_{\rm src}(\lambda))}^{m_{\rm hi}} m \, \frac{dN}{dm} \, dm$$

Plus, useful "resonance" if $R_{\rm ein}(m) \approx R_{\rm src}$.

Many possibilities:

- radio
- mid-IR *(Chiba et al. 2005, Poindexter et al. 2007, Minezaki et al. 2009, Fadely & CRK)*
- optical emission lines *(Moustakas & Metcalf 2003, Metcalf et al. 2004, CRK et al. 2006, Sluse et al. 2007, Sugai et al. 2007, Eigenbrod et al. 2008)*
- optical continuum
- X-ray *(Blackburne et al. 2006, Pooley et al. 2006, 2007, 2009, Kochanek et al. 2007, Morgan et al. 2008, Chartas et al. 2009, Dai et al. 2009)*

# Mass "threshold"

Band corresponds to range of redshifts in current sample.

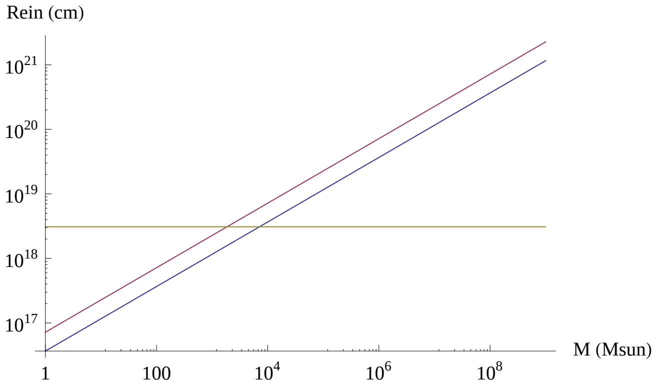

# Milli-images

MG 2016+112, Koopmans et al. (2002)

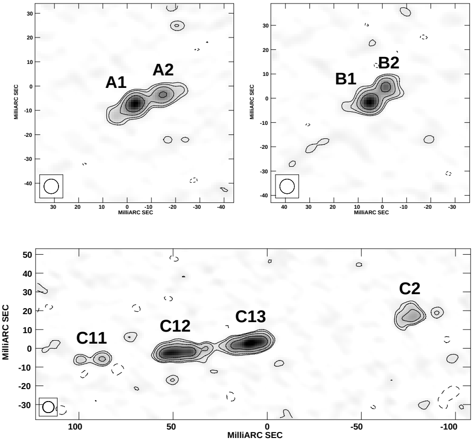

# Milli-images

B0128+437, Biggs et al. (2004)

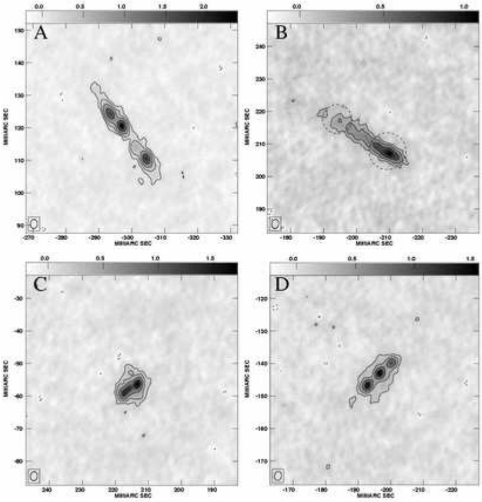

# Milli-images

MG J0414+0534, Trotter et al. (2000)

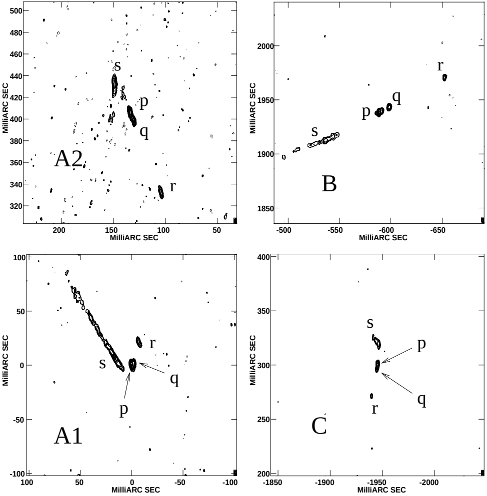

# Gravitational imaging

Vegetti & Koopmans (2009ab): clumps $\gtrsim 10^8\, M_\odot$ visibly perturb Einstein ring images (a la SLACS)

*(my illustration)*

# Time delay millilensing

*(CRK & Moustakas 2009)*

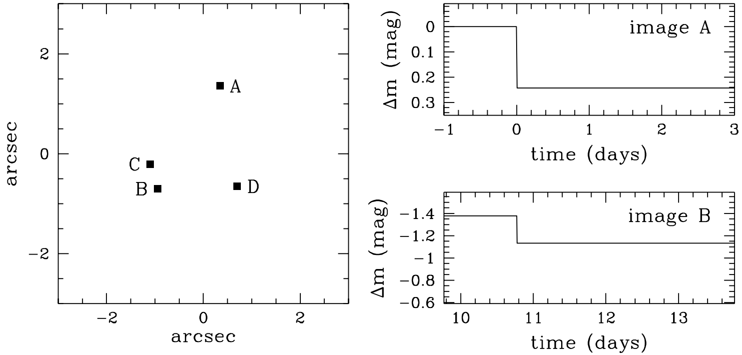

# Time delay millilensing

*(CRK & Moustakas 2009)*

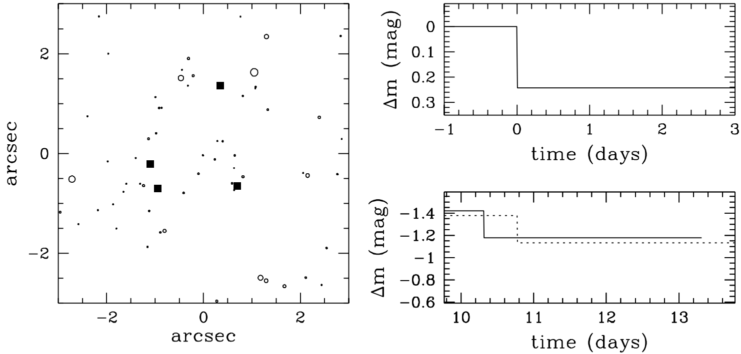

# Time delay millilensing

*(CRK & Moustakas 2009)*

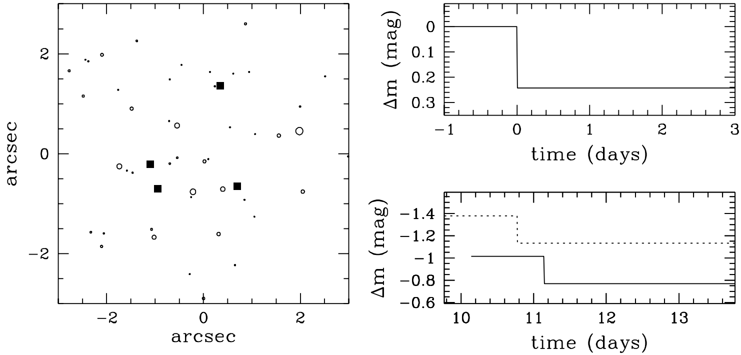

# Time delay millilensing

*(CRK & Moustakas 2009)*

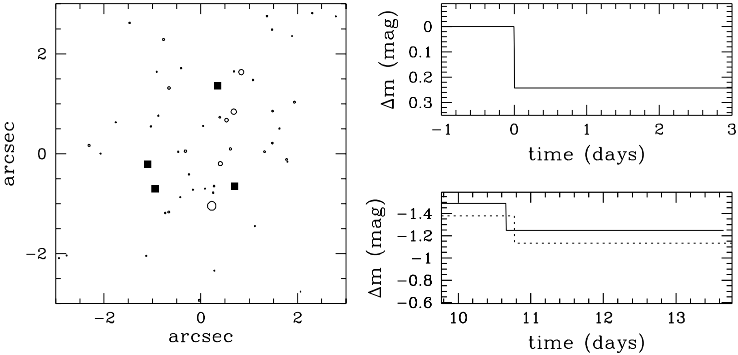

# Time delay millilensing

*(CRK & Moustakas 2009)*

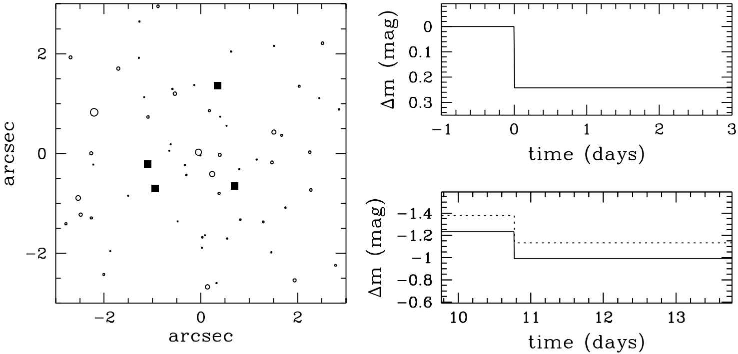

# Random time delays

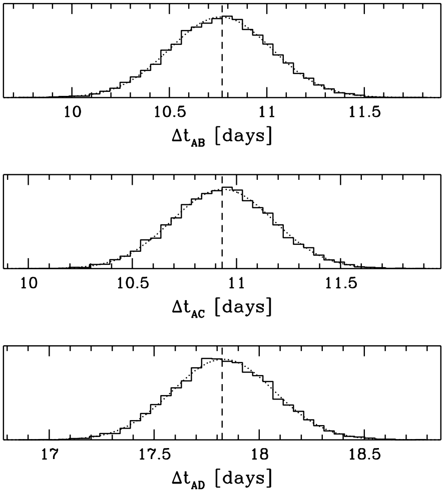

# Scalings

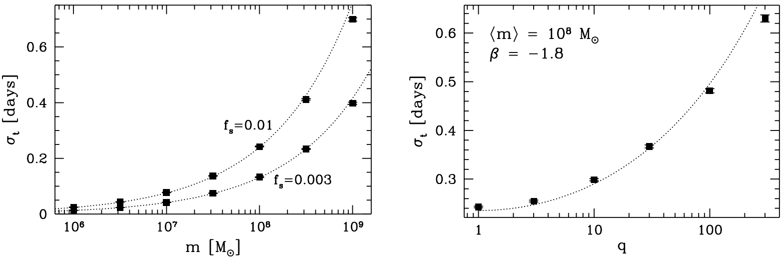


$$\sigma_t \propto \left( f_s \frac{\langle m^2 \rangle}{\langle m \rangle} \right)^{1/2}$$

# RX J1131−1231

Morgan et al. (2006): M2 ($2.2 \pm 1.6$ d) M1 ($9.6 \pm 2.0$ d) S1.

Smooth models predict M1 leads M2.

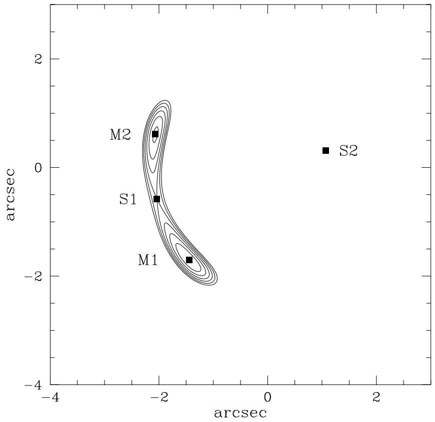

# RX J1131−1231

Morgan et al. (2006): M2 ($2.2 \pm 1.6$ d) M1 ($9.6 \pm 2.0$ d) S1.

But substructure can reverse that ordering. *(CRK & Moustakas 2009)*

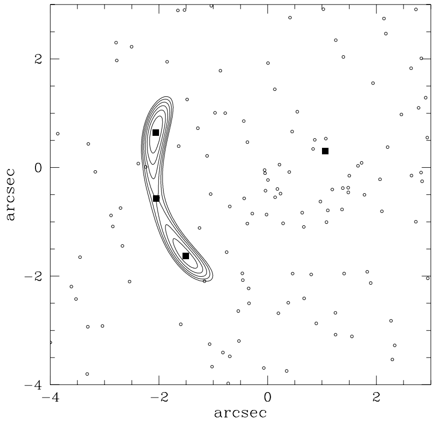

# Summary of observables

- radio flux ratios
- multiwavelength flux ratios
- milli-images
- gravitational imaging
- time delays
- . . . ?

They probe different aspects of the subhalo population . . .
but how, exactly?

# Lensing with stochastic substructure

Can we develop a general theory of substructure lensing?

1. Improve substructure modeling:
   - faster
   - richer — broader substructure models
   - better — understanding of systematic uncertainties
2. Develop general insights:
   - how is information about substructure encoded in lensing observables?
   - what are the “reduced observables” we can/should aim to measure?

# Framework

Lensing potential from 2-d Poisson equation:

$$\nabla^2\phi = 2\kappa = 2\frac{\Sigma}{\Sigma_{\rm crit}}$$

Time delay:

$$\tau(\boldsymbol{x};\boldsymbol{u}) = \frac{1+z_l}{c}\ \frac{D_l D_s}{D_{ls}}\left[\frac{1}{2}\left|\boldsymbol{x}-\boldsymbol{u}\right|^2 - \phi(\boldsymbol{x})\right]$$

Fermat's principle $\nabla_{\boldsymbol{x}}\tau = 0$ gives lens equation:

$$\boldsymbol{u} = \boldsymbol{x} - \boldsymbol{\alpha}(\boldsymbol{x}) \quad \text{where} \quad \boldsymbol{\alpha}(\boldsymbol{x}) = \nabla\phi(\boldsymbol{x})$$

Distortions/magnifications:

$$M = \left(\frac{\partial\boldsymbol{u}}{\partial\boldsymbol{x}}\right)^{-1} = \left[\begin{array}{cc} 1-\phi_{xx} & -\phi_{xy} \\ -\phi_{xy} & 1-\phi_{yy} \end{array}\right]^{-1}$$

# Characterizing substructure effects

Can express observables in terms of

$$
\begin{aligned}
\text{potential} \quad & \phi \\
\text{deflection} \quad \alpha_x &= \frac{\partial \phi}{\partial x} \\
\alpha_y &= \frac{\partial \phi}{\partial y} \\
\text{convergence} \quad \kappa &= \frac{1}{2}\left(\frac{\partial^2 \phi}{\partial x^2} + \frac{\partial^2 \phi}{\partial y^2}\right) \\
\text{shear} \quad \gamma_c &= \frac{1}{2}\left(\frac{\partial^2 \phi}{\partial x^2} - \frac{\partial^2 \phi}{\partial y^2}\right) \\
\gamma_s &= \frac{\partial^2 \phi}{\partial x \partial y}
\end{aligned}
$$

Formally, we need to know the (joint) probability distribution of $\mathbf{\Phi} = \{\phi, \alpha_x, \alpha_y, \kappa, \gamma_c, \gamma_s\}$ at all image positions.

# Deflection

$$\alpha_x = \frac{\partial \phi}{\partial x} \qquad \alpha_y = \frac{\partial \phi}{\partial y}$$

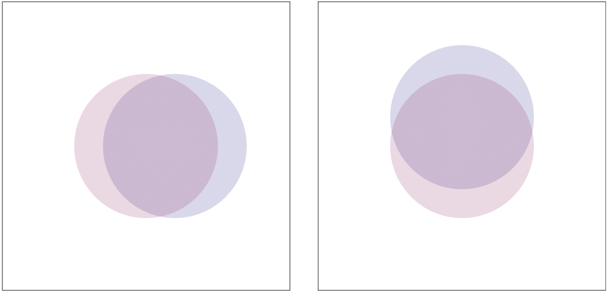

# Convergence

$$\kappa = \frac{1}{2}\left(\frac{\partial^2\phi}{\partial x^2} + \frac{\partial^2\phi}{\partial y^2}\right)$$

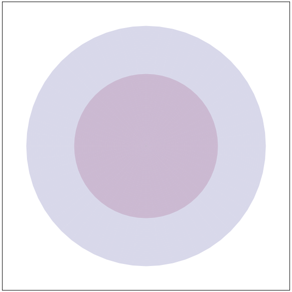

# Shear

$$\gamma_c = \frac{1}{2}\left(\frac{\partial^2\phi}{\partial x^2} - \frac{\partial^2\phi}{\partial y^2}\right) \qquad \gamma_s = \frac{\partial^2\phi}{\partial x \partial y}$$

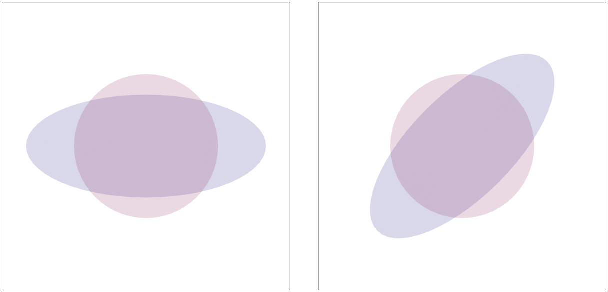

Use polar coordinates $(r_i, \theta_i)$ centered on an image:

$$\begin{aligned}
\phi &= \sum_i \frac{m_i}{\pi} \ln r_i \\
\begin{bmatrix} \alpha_x \\ \alpha_y \end{bmatrix} &= -\sum_i \frac{m_i}{\pi r_i} \begin{bmatrix} \cos\theta_i \\ \sin\theta_i \end{bmatrix} \\
\begin{bmatrix} \gamma_c \\ \gamma_s \end{bmatrix} &= -\sum_i \frac{m_i}{\pi r_i^2} \begin{bmatrix} \cos 2\theta_i \\ \sin 2\theta_i \end{bmatrix}
\end{aligned}$$

(Small corrections for any clump that overlaps line of sight.)

Can we just use the Central Limit Theorem?

Use polar coordinates $(r_i, \theta_i)$ centered on an image:

$$\phi = \sum_i \frac{m_i}{\pi} \ln r_i$$

$$\begin{bmatrix} \alpha_x \\ \alpha_y \end{bmatrix} = -\sum_i \frac{m_i}{\pi r_i} \begin{bmatrix} \cos\theta_i \\ \sin\theta_i \end{bmatrix}$$

$$\begin{bmatrix} \gamma_c \\ \gamma_s \end{bmatrix} = -\sum_i \frac{m_i}{\pi r_i^2} \begin{bmatrix} \cos 2\theta_i \\ \sin 2\theta_i \end{bmatrix}$$

(Small corrections for any clump that overlaps line of sight.)

Can we just use the Central Limit Theorem?
No: variances diverge.

Trouble caused by clump(s) closest to image. If we can handle those, we can use CLT on the bulk of the remaining population.

# Local analysis: Uniform spatial distribution

Goal: find probability distributions for most extreme shear, deflection, and potential.

Work through uniform case analytically for illustration.

$$p_x(\boldsymbol{x}) = \frac{\kappa_s}{N \langle m \rangle}$$

(Over some large but finite area such that $\int p_x(\boldsymbol{x})\ d^2\boldsymbol{x} = 1$.)

Polar coordinates $(r_i, \theta_i)$ centered on an image. Shear strength:

$$\gamma_i = \frac{m_i}{\pi r_i^2}$$

What is the probability distribution for the largest shear?

Probability that the shear from clump $i$ is bigger than $\gamma$:

$$\begin{aligned}
P_i(>\gamma) &= \int_{\frac{m_i}{\pi r_i^2}>\gamma} p_x(\boldsymbol{x}_i)\; p_m(m_i)\; d^2\boldsymbol{x}_i\; dm_i \\
&= \frac{1}{N\langle m\rangle}\int dm\; p_m(m)\int d\theta\int_0^{\left(\frac{m}{\pi\gamma}\right)^{1/2}} dr\; r\; \kappa_s \\
&= \frac{1}{N\langle m\rangle}\int dm\; p_m(m)\times 2\pi\times\frac{1}{2}\left(\frac{m}{\pi\gamma}\right)\kappa_s \\
&= \frac{\kappa_s}{N\gamma}
\end{aligned}$$

Probability that *all* shears are smaller than $\gamma$:

$$P_{\rm all}(<\gamma) = \left(1-\frac{\kappa_s}{N\gamma}\right)^N \to \exp\left(-\frac{\kappa_s}{\gamma}\right) \quad \text{for } N\to\infty$$

This is the cumulative probability distribution for $\gamma_{\rm max}$.

Deflection strength:

$$\alpha_i = \frac{m_i}{\pi r_i}$$

What is the probability distribution for the largest deflection?

Probability that the deflection from clump $i$ is bigger than $\alpha$:

$$\begin{aligned} P_i(>\alpha) &= \int_{\frac{m_i}{\pi r_i}>\alpha} p_x(\boldsymbol{x}_i)\; p_m(m_i)\; d^2\boldsymbol{x}_i\; dm_i \\ &= \frac{1}{N\,\langle m\rangle} \int dm\; p_m(m) \int d\theta \int_0^{\frac{m}{\pi\alpha}} dr\; r\; \kappa_s \\ &= \frac{\kappa_s}{N\pi\alpha^2}\,\frac{\langle m^2\rangle}{\langle m\rangle} \end{aligned}$$

Probability that *all* deflections are smaller than $\alpha$:

$$P_{\rm all}(<\alpha) = \left(1 - \frac{\kappa_s}{N\pi\alpha^2}\,\frac{\langle m^2\rangle}{\langle m\rangle}\right)^N \rightarrow \exp\left(-\frac{\kappa_s}{\pi\alpha^2}\,\frac{\langle m^2\rangle}{\langle m\rangle}\right)$$

# Local analysis: Power law spatial dist'n

Substructure population: $\kappa_s \propto r^{\eta-2}$ with $0 < \eta \leq 2$.

Taylor series expansions for large local shear/deflection:

$$\begin{aligned} P(<\gamma) &= 1 - \frac{\kappa_{s,\mathrm{img}}}{\gamma} \\ &\quad + \frac{\kappa_{s,\mathrm{img}}}{\gamma^2}\left[\frac{\kappa_{s,\mathrm{img}}}{2} - \frac{\langle m^2\rangle}{\langle m\rangle}\frac{(\eta-2)^2}{8\pi r_{\mathrm{img}}^2}\right] + \mathcal{O}\left(\gamma^{-3}\right) \\ P(<\alpha) &= 1 - \frac{\langle m^2\rangle}{\langle m\rangle}\frac{\kappa_{s,\mathrm{img}}}{\pi\alpha^2} \\ &\quad + \frac{\kappa_{s,\mathrm{img}}}{2\pi^2\alpha^4}\left[\frac{\langle m^2\rangle^2}{\langle m\rangle^2}\kappa_{s,\mathrm{img}} - \frac{\langle m^4\rangle}{\langle m\rangle}\frac{(\eta-2)^2}{4\pi r_{\mathrm{img}}^2}\right] + \mathcal{O}\left(\alpha^{-6}\right) \end{aligned}$$

# Mass function: Local shear

$\kappa_s \propto r^{-1}$ and $dN/dm \propto m^{-1.9}$.

Fix $m_{\rm eff} = \langle m^2 \rangle / \langle m \rangle$. Vary $q = m_{\rm hi}/m_{\rm lo} = 1, 10, 100, 1000$.
Theory.

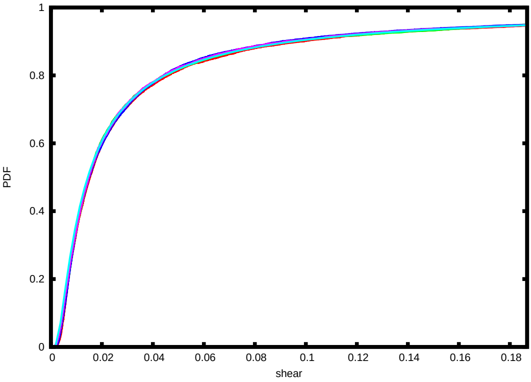

# Mass function: Local shear

$\kappa_s \propto r^{-1}$ and $dN/dm \propto m^{-1.9}$.

Fix $\langle m \rangle$. Vary $q = m_{\rm hi}/m_{\rm lo} = 1, 10, 100, 1000$.

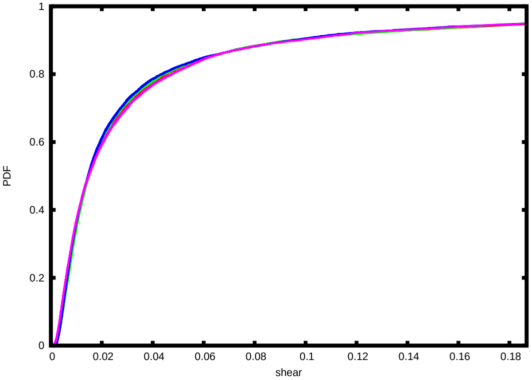

# Mass function: Local deflection

$\kappa_s \propto r^{-1}$ and $dN/dm \propto m^{-1.9}$.

Fix $m_{\rm eff} = \langle m^2 \rangle / \langle m \rangle$. Vary $q = m_{\rm hi}/m_{\rm lo} = 1, 10, 100, 1000$.
Theory.

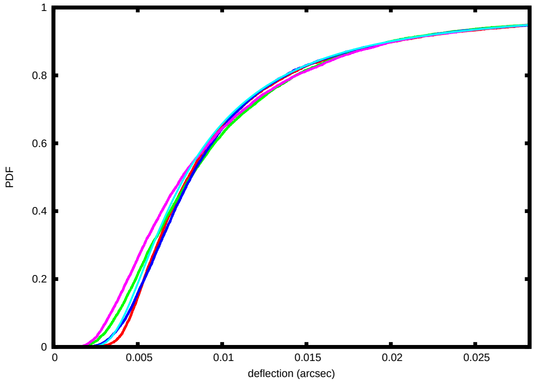

# Mass function: Local deflection

$\kappa_s \propto r^{-1}$ and $dN/dm \propto m^{-1.9}$.

Fix $\langle m \rangle$. Vary $q = m_{\rm hi}/m_{\rm lo} = 1, 10, 100, 1000$.

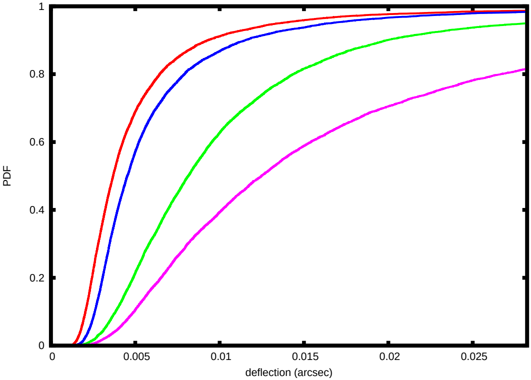

# Mass function: Local potential

$\kappa_s \propto r^{-1}$ and $dN/dm \propto m^{-1.9}$.

Fix $m_{\rm eff} = \langle m^2 \rangle / \langle m \rangle$. Vary $q = m_{\rm hi}/m_{\rm lo} = 1, 10, 100, 1000$.

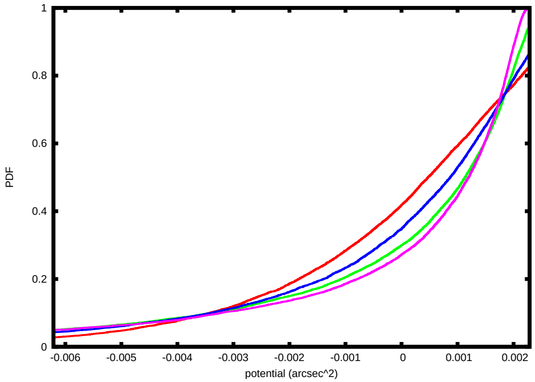

# Spatial distribution: Local shear

$\kappa_s \propto r^{\eta-2}$ and $dN/dm \propto m^{-1.9}$ with $q = 100$.
Isothermal ($\eta = 1$), steeper ($\eta = 0.5$), and shallower ($\eta = 1.5$).

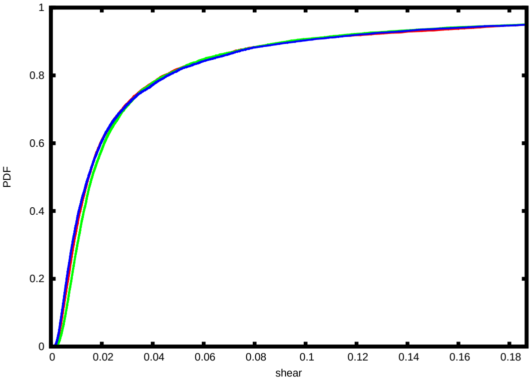

# Spatial distribution: Local deflection

$\kappa_s \propto r^{\eta-2}$ and $dN/dm \propto m^{-1.9}$ with $q = 100$.
Isothermal ($\eta = 1$), steeper ($\eta = 0.5$), and shallower ($\eta = 1.5$).

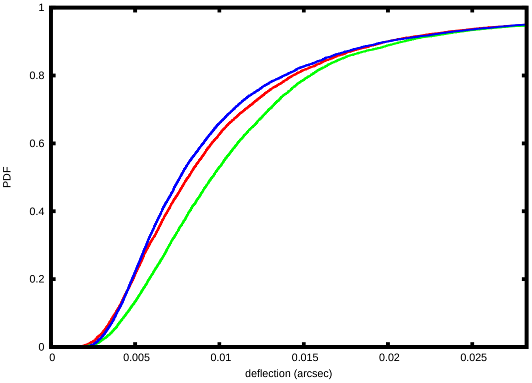

# Spatial distribution: Local potential

$\kappa_s \propto r^{\eta-2}$ and $dN/dm \propto m^{-1.9}$ with $q = 100$.
Isothermal ($\eta = 1$), steeper ($\eta = 0.5$), and shallower ($\eta = 1.5$).

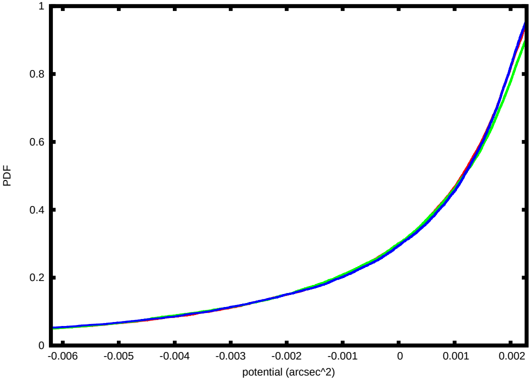

# Long-range analysis

Can use Central Limit Theorem ⇒ need to know variance.

Illustrate with deflection:

$$\alpha_x = \sum_i \alpha_{xi}$$

Variance:

$$\begin{aligned}
\mathrm{var}(\alpha_x) &= \left\langle \alpha_x^2 \right\rangle - \left\langle \alpha_x \right\rangle^2 \\
&= \sum_i \sum_j \left\langle \alpha_{xi} \alpha_{xj} \right\rangle - \left( \sum_i \left\langle \alpha_{xi} \right\rangle \right)^2 \\
&= \sum_i \left\langle \alpha_{xi}^2 \right\rangle + \sum_i \sum_{j \neq i} \left\langle \alpha_{xi} \right\rangle \left\langle \alpha_{xj} \right\rangle - \left( N \left\langle \alpha_{xi} \right\rangle \right)^2 \\
&= N \left\langle \alpha_{xi}^2 \right\rangle - N \left\langle \alpha_{xi} \right\rangle^2
\end{aligned}$$

$$\langle \alpha_{xi} \rangle = \frac{1}{N \langle m \rangle} \int dm_i \; p_m(m_i) \int d^2\boldsymbol{x}_i \; \kappa_s(\boldsymbol{x}_i) \; \frac{m_i \cos\theta_i}{\pi r_i}$$

$$\langle \alpha_{xi}^2 \rangle = \frac{1}{N \langle m \rangle} \int dm_i \; p_m(m_i) \int d^2\boldsymbol{x}_i \; \kappa_s(\boldsymbol{x}_i) \; \left( \frac{m_i \cos\theta}{\pi r_i} \right)^2$$

Note

$$N \langle \alpha_{xi} \rangle^2 \sim \mathcal{O}\left( \frac{1}{N} \right)$$

Thus

$$\mathrm{var}(\alpha_x) \approx N \langle \alpha_{xi}^2 \rangle = \frac{\langle m^2 \rangle}{\langle m \rangle} \int d^2\boldsymbol{x}_i \; \kappa_s(\boldsymbol{x}_i) \left( \frac{\cos\theta}{\pi r_i} \right)^2$$

Similar analysis for all quantities.

# Local vs. total: Shear

$\kappa_s \propto r^{-1}$ and $dN/dm \propto m^{-1.9}$ with $q = 100$.

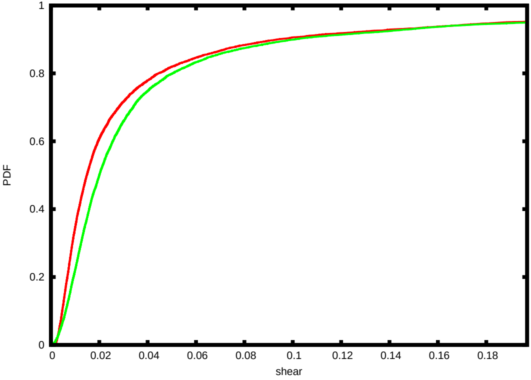

# Local vs. total: Deflection

$\kappa_s \propto r^{-1}$ and $dN/dm \propto m^{-1.9}$ with $q = 100$.

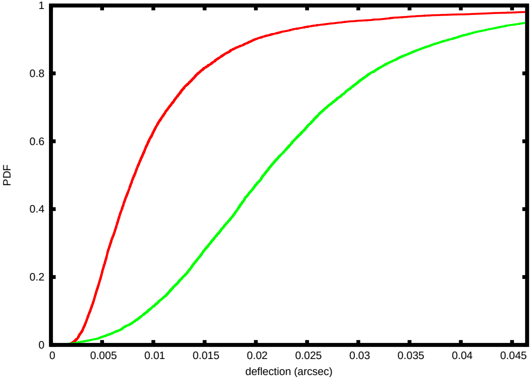

# Local vs. total: Potential

$\kappa_s \propto r^{-1}$ and $dN/dm \propto m^{-1.9}$ with $q = 100$.

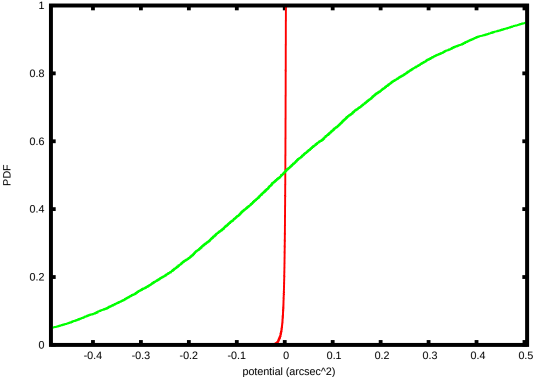

# Mass function: Total shear

$\kappa_s \propto r^{-1}$ and $dN/dm \propto m^{-1.9}$.

Fix $m_{\rm eff} = \langle m^2 \rangle / \langle m \rangle$. Vary $q = m_{\rm hi}/m_{\rm lo} = 1, 10, 100, 1000$.

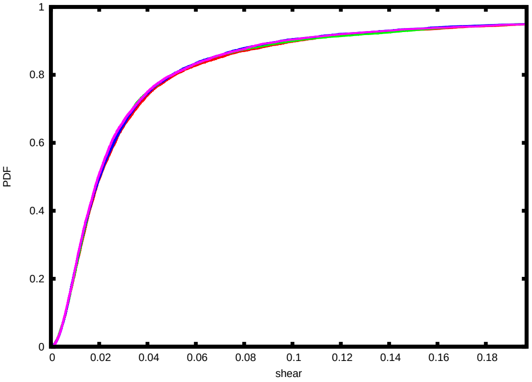

# Mass function: Total deflection

$\kappa_s \propto r^{-1}$ and $dN/dm \propto m^{-1.9}$.

Fix $m_{\rm eff} = \langle m^2 \rangle / \langle m \rangle$. Vary $q = m_{\rm hi}/m_{\rm lo} = 1, 10, 100, 1000$.

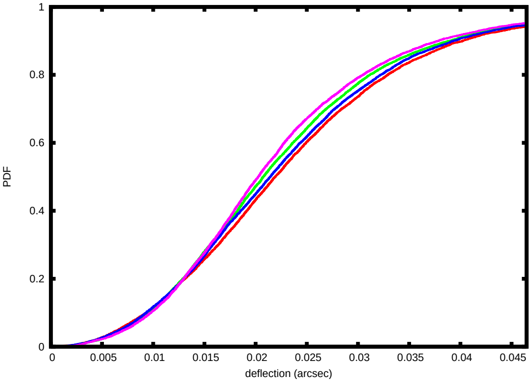

# Mass function: Total potential

$\kappa_s \propto r^{-1}$ and $dN/dm \propto m^{-1.9}$.

Fix $m_{\rm eff} = \langle m^2 \rangle / \langle m \rangle$. Vary $q = m_{\rm hi}/m_{\rm lo} = 1, 10, 100, 1000$.

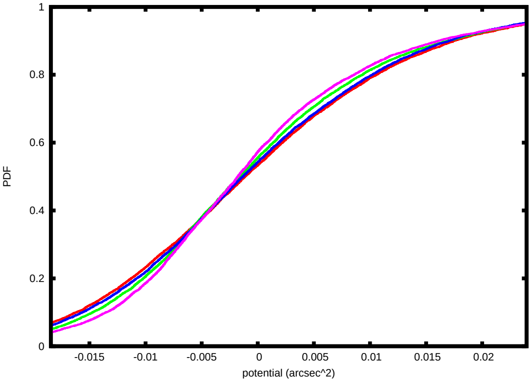

# Spatial distribution: Total shear

$\kappa_s \propto r^{\eta-2}$ and $dN/dm \propto m^{-1.9}$ with $q = 100$.
Isothermal $(\eta = 1)$, steeper $(\eta = 0.5)$, and shallower $(\eta = 1.5)$.

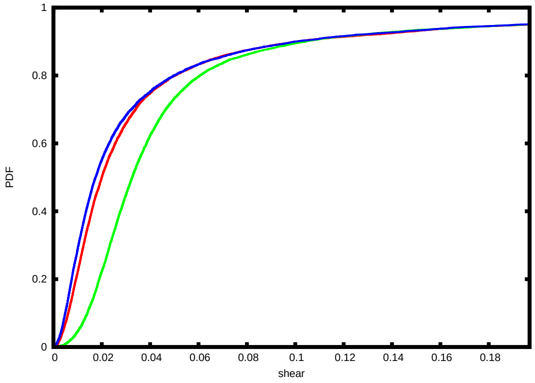

# Spatial distribution: Total deflection

$\kappa_s \propto r^{\eta-2}$ and $dN/dm \propto m^{-1.9}$ with $q = 100$.
Isothermal $(\eta = 1)$, steeper $(\eta = 0.5)$, and shallower $(\eta = 1.5)$.

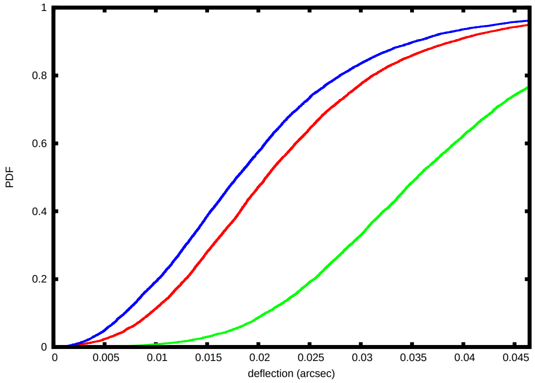

# Spatial distribution: Total potential

$\kappa_s \propto r^{\eta-2}$ and $dN/dm \propto m^{-1.9}$ with $q = 100$.
Isothermal $(\eta = 1)$, steeper $(\eta = 0.5)$, and shallower $(\eta = 1.5)$.

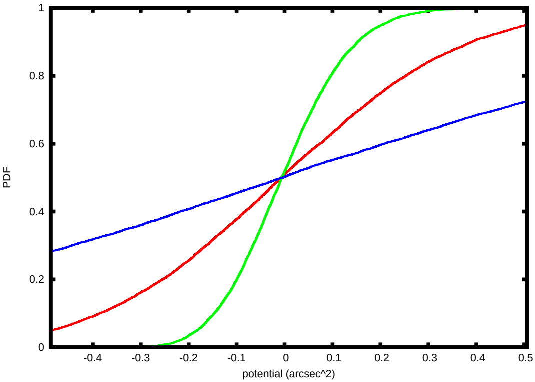

# Lensing Complementarity

Einstein radius, $R_{\rm ein} \propto m^{1/2}$. Scaled distance, $\hat{r} = r/R_{\rm ein}$.

| observable | mnemonic | mass scale | spatial scale |
|---|---|---|---|
| magnifications | $\delta\mu \sim 1/\hat{r}^2$ | $\int m \frac{dN}{dm}\, dm$ | quasi-local |
| positions | $\delta x \sim R_{\rm ein}/\hat{r}$ | $\langle m^2 \rangle / \langle m \rangle$ | intermediate |
| time delays | $\delta t \sim R_{\rm ein}^2 \ln \hat{r}$ | $\langle m^2 \rangle / \langle m \rangle$ | long-range |

Different observables contain different information about the clump population.

# Outlook

| *what* | *how* | *reduced observables* |
|---|---|---|
| mass function | combine observables | $\int m\,(dN/dm)\,dm$ and $\langle m^2\rangle\,/\,\langle m\rangle$ |
| low-mass cutoff (e.g., WDM) | multiwavelength flux ratios | $\int m\,(dN/dm)\,dm$ for different thresholds |
| spatial distribution | time delays | something like $\int r^{-n}\,\kappa_s(\boldsymbol{x})\,d^2\boldsymbol{x}$ |

# Outlook

Radio quads.

- radio loud: 9 — 3 currently have milli-images
- radio quiet: $\gtrsim$20 — doable with EVLA and e-MERLIN?

*(N. Jackson, O. Wucknitz)*

Multiwavelength (optical/IR).

- Others: 4 quads + 1 double published
- Fadely: 1 quad + 5 doubles now, 2 quads + 8 doubles soon

Quad time delays. *(Congdon et al. ApJ submitted)*

- 7 known currently; more and better measurements to come...
- 1 with clear evidence for substructure
- 4 with "anomalies"

Gravitational imaging: $\gtrsim$100 SLACS lenses. *(S. Vegetti et al.)*

# Outlook

Wide-field time-domain surveys will yield thousands of new lenses: Pan-STARRS, DES, LSST, SKA, ...

Dream:

- Clean sample of $\sim$100 quads.
- Radio/mid-IR photometry: multiwavelength flux ratios.
- Radio interferometry: milli-images.
- Optical/near-IR monitoring: precise time delays.
  *(Also microlensing and AGN structure.)*

# Outlook

Wide-field time-domain surveys will yield thousands of new lenses: Pan-STARRS, DES, LSST, SKA, ...

Dream:

- Clean sample of $\sim$100 quads.
- Radio/mid-IR photometry: multiwavelength flux ratios.
- Radio interferometry: milli-images.
- Optical/near-IR monitoring: precise time delays.
  *(Also microlensing and AGN structure.)*

The Observatory for Multi-Epoch Gravitational lens Astrophysics (OMEGA)! *(L. Moustakas et al.)*